Pak. J. Bot., 58(12): December 2026.

ARTICLE DOI: http://dx.doi.org/10.30848/PJB2026-12(11)

GENOME-WIDE IDENTIFICATION OF P-GLYCOPROTEIN (*PGP*/*ABCB*) GENES IN RAPESEED (*BRASSICA NAPUS*) AND THEIR RESPONSES TO PHOSPHATE STARVATION

SANA BASHARAT[1†], WALEED HUSSAIN[†2], ZAHIDA PARVEEN[3], MANSOOR HAMEED[3], PINGWU LIU[1*], MUHAMMAD WASEEM[1*]

[1]School of Breeding and Multiplication (Sanya Institute of Breeding and Multiplication), School of Tropical Agriculture and Forestry, Hainan University, Sanya 572025, China
[2]Department of Botany, University of Narowal, Pakistan
[3]Department of Botany, University of Agriculture Faisalabad, Pakistan
[†]These authors contribute equally

*Corresponding author's email: m.waseem.botanist@gmail.com, drwaseem@hainanu.edu.cn, hnulpw@hainanu.edu.cn

Abstract

Phosphorus (P) starvation severely limits the growth and yield of rapeseed (*Brassica napus*). The ATP-binding cassette B subfamily (ABCB), also known as P-glycoproteins (PGPs), is widely involved in auxin transport and plant abiotic stress responses; however, their role in rapeseed response to low-P stress remains unclear. To our knowledge, the present study is the first comprehensive genome-wide analysis of the ABCB/PGP transporter subfamily in *B. napus*, providing novel insights into their structural diversity, evolutionary expansion, and potential roles in phosphorus starvation responses. In this study, 48 *BnaPGP* genes with conserved ABCB domains were identified and phylogenetically categorized into five major clades, each exhibiting conserved intron–exon structures and motif composition. Chromosomal localization analysis revealed that *BnaPGP* genes are unevenly distributed across 19 chromosomes and exhibit extensive segmental duplication events, suggesting that the expansion of this gene family occurred via gene duplication. Collinearity analysis revealed that the *BnaPGP* genes in rapeseed and *Arabidopsis* shared higher homology than those in *B. rapa* and *B. oleracea*. Promoter *cis*-regulatory element analysis revealed that members of this family possess multiple regulatory elements related to hormone and stress responses. Expression profiling under phosphorus deficiency revealed that multiple *BnaPGP* genes were significantly upregulated in roots, suggesting their potential involvement in root structural remodeling and phosphorus acquisition. Our study provides a foundation and genetic resources for subsequent functional validation and molecular breeding of high-P-efficient rapeseed varieties.

Key words: Transporters; Starvation; Phosphorus; Gene Expression; Root

Introduction

The adenosine triphosphate-binding cassette (ABC) transphyletic protein superfamily is ubiquitous and encodes membrane-bound transporter proteins that facilitate inter/intracellular transportation across membranes (Aslam *et al.*, 2021; Devi *et al.*, 2024). The ABC protein comprises a hydrophobic transmembrane domain (TMD) and a peripheral nucleotide-binding domain (NBD), forming either full-sized or half-sized ABC proteins (Aslam *et al.*, 2021). Further classification of the superfamily is based on the positional arrangement and spatial orientation of the TMD-NBD domain into ABCA to ACBI subfamilies, excluding ABCH. In plants, the ABCB subfamily encodes full-size (TMD–NBD–TMD–NBD) and half-size transporters (TMD–NBD) with a typical domain arrangement of two TMDs and two NBDs (Yan *et al.*, 2017). Plant ABCBs are sometimes referred to as P-glycoproteins (PGPs) because of their structural similarity to animal P-glycoproteins (Xu *et al.*, 2014b). PGPs have garnered particular interest because of the participation of members of the PGP subfamily in phytohormone transport and regulation, secondary metabolite distribution, cellular detoxification, and abiotic stress responses *(Dahuja et al.*, 2021).

PGP transporters play pivotal roles in polar auxin transport, functioning alongside PIN-FORMED (PIN) and AUXIN1/LIKE-AUXIN (AUX1/LAX) transporters, with PGPs being particularly important for auxin movement in apical tissues and over long distances (Blakeslee *et al.*, 2007). In *Arabidopsis*, six of the 22 ABCBs–ABCB1, ABCB4, ABCB6, ABCB19, ABCB20, and ABCB21 (Kang *et al.*, 2011)–participate in auxin transport. For instance, AtABCB1 (root-expressed) and AtABCB19 (plasma membrane-localized) mediate auxin efflux (Titapiwatanakun *et al.*, 2008), AtABCB4 regulates auxin influx in root epidermal cells to promote root hair formation and lateral root development (Santelia *et al.*, 2005), and AtABCB6 and AtABCB20 have redundant functions (Zhang *et al.*, 2018). AtABCB21 maintains pericycle auxin levels for sustained transport toward the leaf tip, and its loss reduces root auxin delivery and delays lateral root formation (Jenness *et al.*, 2020). In crops, ABCB transporters display conserved and stress-responsive functions. In maize, *ZmABCB15* facilitates polar auxin transport and enhances resistance to Rice black-streaked dwarf virus (RBSDV) by reducing viral replication (Yue *et al.*, 2022), while *BRACHYTIC 2* (*BR2*), homologous to *AtABCB1*, regulates basipetal auxin

Received: 29-01-2026 Revised: 02-04-2026 Accepted: 08-04-2026 Online: 03-07-2026

transport, with mutations causing dwarfism (Multani *et al*., 2003). *ZmABCB7* and *ZmABCB8* are drought-inducible, whereas *ZmABCB18* is suppressed by salt stress (Pang *et al*., 2013). In rice, knockout lines of plasma membrane-localized *OsABCB14* exhibit reduced auxin levels, impaired polar auxin transport, and insensitivity to iron deficiency (Xu *et al*., 2014a). Other rice ABCBs, including *OsABCB8*, *OsABCB11*, *OsABCB13*, *OsABCB23*, and *OsABCB24*, are upregulated by drought, whereas *OsABCB6*, *OsABCB9*, and *OsABCB8* respond to salt stress (Saha *et al*., 2014). ABCB transporters also mediate the response to heavy metals. For example, ATM3/AtABCB24 is induced by Cadmium (Cd) and lead (Pb), conferring tolerance (Kim *et al*., 2006a), whereas ALS1/TAP2 (*AtABCB27*) is involved in Al transport (Larsen *et al*., 2007). Collectively, PGP transporters are integral to auxin transport, abiotic stress tolerance, and diverse developmental processes in plant species.

Phosphorus (P) is an essential macronutrient in plants, playing a pivotal role in growth, development, and overall productivity, including that of rapeseed (Liu *et al*., 2024). Plants required adequate P supply to maintain an optimal root system architecture, promote water and nutrient use efficiency, enhance seedling establishment, and improve plant vigor and overall plant biomass accumulation (Ren *et al*., 2012; Yang *et al*., 2012; Adu *et al*., 2017). In rapeseed, during the vegetative to reproductive growth transition, an optimal level of P accelerates flowering, increases siliques per plant, promotes seed set, improves pollen viability, and enhances fertilization efficiency (Duan *et al*., 2020; Zhang *et al*., 2025b). Starvation of P leads to reduced branching, delayed flowering, and lower assimilate partitioning to reproductive organs, ultimately decreasing the yield potential (Li *et al*., 2023; Zhang *et al*., 2023). *Brassica napus* is an important edible oil crop that is sensitive to P starvation. An optimal amount of P is required for high seed yields and oil content. Currently, rapeseed is suffering from constant P deficiency. Therefore, it is essential to breed rapeseed cultivars with enhanced P-use efficiency, high yield, and high productivity. Given that PGP transporters are broadly involved in the uptake and distribution of plant nutrients, it is highly likely that members of the PGP subfamily participate in plant responses to P starvation.

ABC superfamily members play pivotal roles in P uptake and translocation in plants (Aslam *et al*., 2021). Recent advances in genomic and bioinformatic approaches have facilitated the genome-scale discovery of a vast array of ABC transporter proteins in diverse plant species such as *Arabidopsis*, soybean, tomato, rice, pepper, pineapple, and lotus (Aslam *et al*., 2021; Devi *et al*., 2024; Xu *et al*., 2014b). The subfamily PGP is second largest ABC protein family following PGP in plants (Aslam *et al*., 2021) with 28 members in *Arabidopsis* (Jasinski *et al*., 2003), 39 members in *Brassica rapa* (Yan *et al*., 2017), 29 members in *Paeonia ostii* (Shang *et al*., 2025), 22 members in rice (Xu *et al*., 2014b), 45 members in *Glycyrrhiza glabra* (Devi *et al*., 2024), 39 genes in soybean (Zou *et al*., 2025), 19 members in grapevine (Çakır *et al*., 2023), 31 members in maize (Pang *et al*., 2013), 48 in *Linum usitatissimum* (Khan *et al*., 2020), and 29 members in tomatoes (Ofori *et al*., 2018). To date, PGP family members in rapeseed have not been characterized to explore their role in P starvation. The present study reports the *in silico* identification of the PGP transporter subfamily in rapeseed using different bioinformatics tools. Furthermore, the putative roles of selected BnaPGP family members were elucidated in rapeseed under phosphorus starvation.

Materials and Methods

Mining of PGP proteins in rapeseed: Two complementary approaches were adopted to identify members of the PGP gene family in rapeseed. First, the protein sequences of the Arabidopsis PGP subfamily members (Jasinski *et al*., 2003) were downloaded from the TAIR database (https://www.arabidopsis.org/) and used as a BLASTP query against the entire rapeseed proteome (vZS11). Second, the PGP PFAM domain pattern (PF00005, nucleotide-binding domain (NBD), and PF00664, transmembrane domain (TMD)) was downloaded from the Pfam database (https://pfam.xfam.org/) and used in the HMMsearch algorithm (E-value: 1×10^{-5}) to identify potential PGP protein members in the rapeseed proteome. The results of both analyses were combined to avoid redundancy. The PGP domain was verified using the NCBI Conserved Domain Database (CDD; https://www.ncbi.nlm.nih.gov/ Structure/ index.shtml) and further validated using SMART (http://smart.embl-heidelberg.de/smart/batch.pl). The putative PGP subfamily genes were renamed in ascending order on rapeseed chromosomes (*BnaA.PGP1* to *BnaA.PGP20*, sub-genome A; *BnaC.PGP21* to *BnaC.PGP43*, sub-genome C; *Bna.PGP44* to *Bna.PGP48*, on scaffold).

The characteristic features of PGP protein members, such as their molecular weight (MW, kDa), isoelectric point (pI), and hydrophobicity index, were assessed using the Sequence Manipulation Suite (https://www.bioinformatics.org/sms2/). The *BnaPGP* protein along with peptide sequences from Arabidopsis and soybean were aligned using ClustalO (https://www.ebi.ac.uk/Tools/msa/clustalo/). Subsequently, the resultant multiple sequence alignment was used to construct an unrooted maximum-likelihood tree using IQ-TREE and bootstrap with 1000 replicates. Moreover, *in silico* subcellular localization prediction analysis of each BnaPGP protein was performed using WoLF–PSORT (https://wolfpsort.hgc.jp/).

PGP gene structure analysis in rapeseed: The positions of PGP domains within the protein sequences were predicted using the NCBI Conserved Domain Database (CDD), as previously described for the mining of PGP proteins in rapeseeds. The intron–exon structures of the rapeseed PGP genes were retrieved from the genome annotation files. Conserved motif prediction was performed using the MEME Suite (https://meme-suite.org/meme/tools/meme), with peptide sequences submitted under the following parameters: (*i*) maximum number of motifs set to 10, (*ii*) optimal motif width between 10 and 50 residues, and (*iii*) motif repetition set to 'any.' The outputs generated from the above-mentioned tools were used to visualize PGP protein features using the Gene Structure View module in TBtools. To identify cis-*acting* regulatory elements (CAREs) within promoter regions (defined as the 2000 bp upstream of the transcription start site), the PlantCARE database (http://bioinformatics.psb.ugent.be/webtools/plantcare/html/) was used. Predicted CAREs were visualized using TBtools.

PGP gene chromosome location and duplication in rapeseed genome: The PGP gene locations on chromosomes were obtained from the rapeseed genome annotation file. PGP gene duplication events were analyzed using MCScanX (https://github.com/wyp1125/MCScanX). The syntenic map with chromosome location and PGP duplications was visualized in the CIRCOS plot using TBtools. Ka/Ks ratios of paralogous gene pairs for all duplication pairs were calculated using the Ks_Ka calculator – tbtools.

Plant growth conditions, treatment, and sample collection: Seeds of the rapeseed inbred line 383-5 were surface-sterilized and germinated under controlled growth room conditions (24°C, 16 h light/8 h dark photoperiod). The seeds were placed on moistened gauze in a light incubator with an illumination intensity of 40 μmol $m^{-2}·s^{-1}$. Water was sprayed daily to maintain the moisture of the gauze.

Following germination, the seedlings were transplanted into 12-hole trays filled with perlite. Each tray received 300 mL of 1/4-strength Hoagland nutrient solution (pH 6.0, EC 1.2 $mS·cm^{-1}$). The nutrient solution was replaced every two days, and the growth substrate was thoroughly washed with pure water every 10 days to maintain the stability of the nutrients.

After two months of cultivation, 60 healthy and uniform seedlings were randomly selected for low phosphorus (P) treatments, following Zhang *et al.*, (2024) with slight modifications. For treatment application, the nutrient solution in each tray was replaced with a modified Hoagland solution containing: 4 $mmol·L^{-1}$ $Ca(NO_3)_2$, 0.2 $μmol·L^{-1}$ $CuSO_4$, 2 $mmol·L^{-1}$ Fe(Na)EDTA, 50 $μmol·L^{-1}$ H_3BO_3, 6 $mmol·L^{-1}$ KNO_3, 2 $mmol·L^{-1}$ $MgSO_4$, 2 $μmol·L^{-1}$ KCl, 4 $μmol·L^{-1}$ $MnSO_4$, 0.2 $μmol·L^{-1}$ $(NH_4)_6Mo_7O_{24}$, and 4 $μmol·L^{-1}$ $ZnSO_4$. Phosphorus levels were adjusted by adding $NH_4H_2PO_4$ to achieve a low-P concentration of 0.125 $mmol·L^{-1}$. To compensate for the removal of ammonium (NH_4^+) and avoid low-nitrogen stress, 1 $mol·L^{-1}$ NH_4Cl was added.

The control treatment (CK) consisted of the same modified Hoagland solution containing 1.000 $mmol·L^{-1}$ P. A total of 24 seedlings were allocated to each group. Plant samples were collected after 20 days of low phosphorus treatment, immediately frozen in liquid nitrogen, and stored at −80°C for subsequent analyses.

Nucleic acid extraction and RT-qPCR analysis: To analyze PGP gene expression in rapeseeds, total RNA was extracted from all selected samples using TRIZOL reagent, following the manufacturer's instructions. The concentration of extracted RNA was quantified using a NanoDrop spectrophotometer (Thermo Fisher Scientific, USA), and RNA quality was assessed by 2% (w/v) agarose gel electrophoresis. Prime Script ™ RT reagent Kit with gDNA Eraser (Takara, JAPAN) was used to synthesize first cDNA strand. For gene expression analysis, RT-qPCR was performed by running reaction system prepared with SYBR-Premix Ex Taq-II (TliRNaseH Plus) on CFX96 Touch ™ Real-Time PCR Detection System (BIO-RAD, USA) following the provided protocol. The *BnACTIN7* (GenBank accession no. AF024716) was used as an internal reference gene to normalize gene expression. The $2^{-\Delta\Delta Ct}$ method (Livak & Schmittgen, 2001) was used to calculate the relative expression of the selected BnaPGP genes. All reactions were conducted with three biological replicates, each comprising three technical replicates. The primers used in this study are listed in Table 1.

Table 1. All the primers used in present study.

Sequence ID	Primer ID	Primer sequence	Primer Tm	Product size
BnaA.ABCB1	BnaA.ABCB1_1_F	GCGCTTGTGGGACAGAGT	59.969	81
BnaA.ABCB1	BnaA.ABCB1_1_R	TTTTCCTGCGGTCGGGTC	59.969	81
BnaA.ABCB4	BnaA.ABCB4_1_F	CGGTTTTAGCGCGGATGC	59.977	109
BnaA.ABCB4	BnaA.ABCB4_1_R	CACCTTGTCCTCTGCGCA	59.969	109
BnaA.ABCB6	BnaA.ABCB6_1_F	ATGCCAAGGGGACACAGC	59.964	113
BnaA.ABCB6	BnaA.ABCB6_1_R	AGGTGGCTCGAGGTTTGC	59.967	113
BnaA.ABCB10	BnaA.ABCB10_1_F	TGCGTGGTACGGAAGCAG	60.049	150
BnaA.ABCB10	BnaA.ABCB10_1_R	GCTGCTGCAACTGAAGCC	59.742	150
BnaA.ABCB14	BnaA.ABCB14_1_F	CGCCGTTGTAGTCGAGCA	60.127	149
BnaA.ABCB14	BnaA.ABCB14_1_R	CGAGACCAAGCCCTGTGG	60.047	149
BnaA.ABCB19	BnaA.ABCB19_1_F	AACGAGAACGCGTCGGAG	60.127	104
BnaA.ABCB19	BnaA.ABCB19_1_R	TCACCCACGTGCGTCTTG	60.28	104
BnaC.ABCB25	BnaC.ABCB25_1_F	CTGGACAAGCTGCAGCCT	59.966	149
BnaC.ABCB25	BnaC.ABCB25_1_R	ATCTGGCCTCGCAGGGTA	60.042	149
BnaC.ABCB29	BnaC.ABCB29_1_F	ATGCCAAGGGGACACAGC	59.964	113
BnaC.ABCB29	BnaC.ABCB29_1_R	AGGTGGCTCGAGGTTTGC	59.967	113
BnaC.ABCB38	BnaC.ABCB38_1_F	GAGCAAGGCCCTGAGCTC	60.125	146
BnaC.ABCB38	BnaC.ABCB38_1_R	CGCCAGCGTACCAGAACA	60.049	146
BnaC.ABCB42	BnaC.ABCB42_1_F	TGGAACGGTCCTCGCAAC	59.97	101
BnaC.ABCB42	BnaC.ABCB42_1_R	TTGCCACGATCTTGCCGT	59.968	101
Bna.ABCB45	Bna.ABCB45_1_F	ACCCGGACGGAGCTTACT	59.963	107
Bna.ABCB45	Bna.ABCB45_1_R	TCGTTCCGGCAAGGGTTC	59.969	107
Bna.ABCB47	Bna.ABCB47_1_F	ACCCGGACGGAGCTTACT	59.963	107
Bna.ABCB47	Bna.ABCB47_1_R	TCGTTCCGGCAAGGGTTC	59.969	107

Results

Characteristics of *PGP* gene family members in rapeseed: To identify PGP gene family members in rapeseed, we performed BLASTp searches combined with conserved domain identification, ultimately identifying a total of 48 ***BnaPGP*** candidate genes, all of which possessed the typical conserved features of the ABC transporter B subfamily. The genes were named based on their position on chromosomes in ascending order, for instance, *BnaA.PGP1* to *BnaA.PGP20* on sub-genome A, *BnaC.PGP21* to *BnaC.PGP43* on sub-genome C, and those on the scaffold were named as *Bna.PGP44 to Bna.PGP48. BnaPGP* proteins ranged in length from 600 amino acids / 66.8 kDa (BnaC.PGP27) to 1408 amino acids/155.6 kDa (BnaA.PGP9). Theoretical pI values ranged from 5.0 (BnaC.PGP26) to 9.3 (BnaA.PGP18), with 21 proteins having pI values greater than 7.0, suggesting a potential positive charge at neutral pH. The protein instability indices ranged from 31.8 (BnaA.PGP20) to 53.4 (BnaC.PGP26), with approximately 60% having instability indices greater than 40, indicating that they may have low intracellular stability and require specific conditions for function. GRAVY values ranged from 0.0 to 0.3, with most proteins showing positive values, indicating a moderate degree of hydrophobicity. *In silico* subcellular localization analysis revealed that all ***BnaPGP*** proteins were localized to the plasma membrane, consistent with their function as membrane transporters. To further elucidate the functional characteristics of these ***BnaPGP*** proteins, we systematically analyzed their genomic localization, including chromosomal distribution, gene start, and end coordinates (Table 2). Overall, the ***BnaPGP*** family members exhibited strong consistency in their physicochemical properties, suggesting a degree of functional conservation.

Phylogeny of *BnaPGP* with *arabidopsis* and soybean: To further elucidate the evolutionary relationships of *PGP* transporters in rapeseed and other plant species, a multispecies phylogenetic tree was constructed, including *Arabidopsis* and soybean (Fig. 1). Our results showed that PGP family members can be divided into five major groups (I–V). Group I includes genes such as *BnaA.PGP11*, *BnaA.PGP16*, *BnaC.PGP29*, *BnaC.PGP38*, *BnaC.PGP27*, *BnaC.PGP23*, *BnaA.PGP6* and *BnaA.PGP2* is primarily from rapeseed, suggesting a highly conserved evolutionary pattern. Group II, consisting of *BnaA.PGP3*, *BnaA.PGP18*, *BnaA.PGP19*, *BnaC.PGP21*, *BnaC.PGP32*, *BnaC.PGP33*, *BnaPGP45*, *BnaPGP46*, *BnaPGP47*, and *BnaPGP48* have fewer members and may have undergone a degree of functional divergence during evolution. Group III is the largest group, including *BnaA.PGP4*, *BnaA.PGP7*, *BnaA.PGP8*, *BnaA.PGP12*, *BnaA.PGP13*, *BnaA.PGP14*, *BnaA.PGP17*, *BnaA.PGP20*, *BnaC.PGP25*, *BnaC.PGP30*, *BnaC.PGP31*, *BnaC.PGP34*, *BnaC.PGP35*, *BnaC.PGP36*, *BnaC.PGP40*, *BnaC.PGP41*, *BnaC.PGP43* and *Bna.PGP44*, which is widely distributed in various species and undergone significant expansion events. Group IV includes *BnaC.PGP22*, *BnaC.PGP30*, *BnaC.PGP37*, *BnaC.PGP39* and *BnaC.PGP42* is showing specific clustering characteristics. Group V members included *BnaA.PGP5*, *BnaC.PGP26*, *BnaC.PGP27*, and *BnaC.PGP28*, suggesting their possible conserved functions.

Gene structure analysis of *BnaPGP* genes: To further elucidate the evolutionary relationship between *BnaPGP* and gene structure, we integrated phylogeny with intron-exon distribution, domain organization, and conserved motif patterns. Analysis of conserved domains revealed that *BnaPGP* proteins contain two TMD–NBD domains in all phylogenetic clades, with exceptions. For instance, *BnaA.PGP18*/*BnaC.PGP33* in Group II, *BnaA.PGP4*/*BnaA.PGP8* in Group III, and *BnaC.PGP37*/*BnaC.PGP42* in Group IV has one additional domain. Gene structure analysis revealed substantial variation in the number of introns among *BnaPGP* family members in rapeseed, with intron counts ranging from 2 to 12. Group-specific patterns were observed, with Group I containing 2–10 introns, Group II containing 8–12 introns, Group III containing 10–12 introns, Group IV containing 5–9 introns, and Group V containing 3–11 introns. This variation in intron number suggests structural diversification among gene family members, which may contribute to their functional differentiation and regulatory complexity in *R. sativus*.

Conserved motifs in the *BnaPGP* family proteins were analyzed using the MEME Suite, resulting in the prediction of ten distinct motifs (motifs 1– 10). Motif analysis revealed that Motifs 1, 2, 3, 4, 6, 7, and 10 were primarily associated with the NBD regions, reflecting ATP-binding and hydrolysis functions, whereas Motifs 5, 8, and 9 were located within the TMD regions, which are critical for substrate recognition and membrane integration. In addition, the number and distribution of conserved motifs varied across the different phylogenetic groups. These motif distribution patterns were generally consistent with the phylogenetic classification and may reflect clade-specific functional differentiation within the *BnaPGP* family members. In Group I, all members contained ten motifs, except *BnaA.PGP6*, which had only six motifs. Most members of this group carried two copies of Motifs 1, 6, and 9. For instance, *BnaA.PGP2*, *BnaC.PGP23*, and *BnaC.PGP29* each had duplicated Motifs 1, 6, and 9, whereas *BnaA.PGP11*, *BnaA.PGP16*, and *BnaC.PGP38* contained two copies of Motifs 6 and 9. Notably, *BnaC.PGP38* lacked Motif 8. Members of Groups II and IV generally possessed all ten motifs. However, both groups exhibited two copies of Motif 9, and *BnaC.PGP42* uniquely carried two additional copies of Motif 10. Similar to Group I, Group V members contained all ten motifs, with some exceptions. *BnaC.PGP26* lacked motifs 1, 4, 8, and 10, whereas *BnaC.PGP27* retained only motifs 1, 4, 5, 6, 7, and 9. In Group III, most members carried all ten motifs, although *BnaA.PGP7*, *BnaA.PGP44*, *BnaA.PGP8*, *BnaA.PGP14*, *BnaC.PGP25*, *BnaC.PGP30*, *BnaC.PGP35*, and *BnaC.PGP44* lacked Motif 1 but carried two copies of Motif 9. Additionally, some members, including *BnaA.PGP15*, *BnaA.PGP20*, *BnaC.PGP31*, and *BnaC.PGP41*, contained all ten motifs but also displayed duplications of motifs 9 and 10. *BnaC.PGP43* showed duplication of motif 6. Overall, motif analysis demonstrated both conservation and diversification within the *BnaPGP* gene family, with certain members exhibiting unique motif losses or duplications (Fig. 2).

Table 2. Characteristics of *BnaPGP* genes in rapeseed.

Gene ID	Gene name	Protein length (aa)	Instability index	pI*	Molecular weight	Gravy	*In-silico* subcellular localization	Chromosome	Start	End	Strand
BnaA01T0154600ZS	BnaA.PGP1	1275	34.4	9.0	140.4	0.1	Plasma membrane	A01	9115540	9121593	+
BnaA03T0176600ZS	BnaA.PGP2	1339	37.5	7.3	146.7	0.0	Plasma membrane	A03	9057683	9063283	+
BnaA03T0192900ZS	BnaA.PGP3	1403	48.9	6.0	154.9	0.1	Plasma membrane	A03	10015842	10022069	-
BnaA03T0445100ZS	BnaA.PGP4	1257	37.9	6.4	136.2	0.1	Plasma membrane	A03	24149631	24154985	+
BnaA04T0042400ZS	BnaA.PGP5	1400	48.2	5.6	154.3	0.1	Plasma membrane	A04	2890729	2897179	+
BnaA04T0236900ZS	BnaA.PGP6	677	36.0	9.0	74.5	0.0	Plasma membrane	A04	22216240	22219224	+
BnaA04T0296500ZS	BnaA.PGP7	1287	36.1	6.8	138.9	0.1	Plasma membrane	A04	25419935	25425311	-
BnaA05T0008800ZS	BnaA.PGP8	1292	35.2	6.0	139.5	0.1	Plasma membrane	A05	570371	576001	+
BnaA05T0066000ZS	BnaA.PGP9	1408	49.4	5.7	155.6	0.1	Plasma membrane	A05	3613587	3620469	+
BnaA06T0368200ZS	BnaA.PGP10	1241	34.8	8.7	136.5	0.1	Plasma membrane	A06	43684254	43692407	-
BnaA06T0375000ZS	BnaA.PGP11	1252	34.9	8.1	136.7	0.1	Plasma membrane	A06	44130560	44137287	+
BnaA07T0024900ZS	BnaA.PGP12	1249	35.8	6.8	135.5	0.2	Plasma membrane	A07	2137421	2143008	+
BnaA07T0215100ZS	BnaA.PGP13	1254	33.1	7.0	136.3	0.2	Plasma membrane	A07	22348626	22355122	+
BnaA07T0219300ZS	BnaA.PGP14	1292	36.7	6.4	139.8	0.1	Plasma membrane	A07	22567494	22573659	-
BnaA08T0321900ZS	BnaA.PGP15	1276	34.6	7.3	137.1	0.2	Plasma membrane	A08	28309359	28314737	-
BnaA09T0042700ZS	BnaA.PGP16	1252	36.5	8.6	136.7	0.1	Plasma membrane	A09	2657730	2665111	-
BnaA09T0208300ZS	BnaA.PGP17	1234	37.9	7.8	134.6	0.2	Plasma membrane	A09	14507169	14512448	-
BnaA09T0426500ZS	BnaA.PGP18	1256	33.9	9.3	137.2	0.1	Plasma membrane	A09	48752509	48760415	-
BnaA09T0427600ZS	BnaA.PGP19	1239	36.5	9.0	134.3	0.1	Plasma membrane	A09	48822124	48827028	+
BnaA10T0012300ZS	BnaA.PGP20	1284	31.8	8.1	138.1	0.1	Plasma membrane	A10	686050	691645	+
BnaC01T0196000ZS	BnaC.PGP21	1234	33.4	9.2	135.6	0.1	Plasma membrane	C01	14505715	14512221	+
BnaC02T0469200ZS	BnaC.PGP22	1245	39.2	8.2	136.0	0.1	Plasma membrane	C02	57497220	57502392	-
BnaC03T0206500ZS	BnaC.PGP23	1341	37.8	7.3	147.0	0.0	Plasma membrane	C03	12003400	12008910	+
BnaC03T0226400ZS	BnaC.PGP24	1396	49.4	5.9	154.3	0.1	Plasma membrane	C03	13561348	13568662	-
BnaC04T0010000ZS	BnaC.PGP25	1293	35.0	6.3	139.6	0.1	Plasma membrane	C04	1162757	1167850	+

Table 2. (Cont'd.).

Gene ID	Gene name	Protein length (aa)	Instability index	pI*	Molecular weight	Gravy	*In-silico* subcellular localization	Chromosome	Start	End	Strand
BnaC04T0073200ZS	BnaC.PGP26	779	53.4	5.0	85.9	0.0	Plasma membrane	C04	6401198	6405464	+
BnaC04T0073300ZS	BnaC.PGP27	600	44.9	9.1	66.8	0.3	Plasma membrane	C04	6405548	6407616	+
BnaC04T0317300ZS	BnaC.PGP28	1399	49.5	5.7	154.4	0.1	Plasma membrane	C04	42917372	42923650	-
BnaC04T0552400ZS	BnaC.PGP29	1338	37.7	8.0	146.6	0.0	Plasma membrane	C04	66929049	66934944	+
BnaC04T0613600ZS	BnaC.PGP30	1284	35.3	7.0	138.5	0.1	Plasma membrane	C04	70836356	70841778	-
BnaC05T0014300ZS	BnaC.PGP31	1284	32.3	8.5	138.0	0.1	Plasma membrane	C05	966787	972474	+
BnaC05T0239100ZS	BnaC.PGP32	1031	34.9	9.1	111.8	0.0	Plasma membrane	C05	18507570	18512370	-
BnaC05T0240400ZS	BnaC.PGP33	1255	34.3	9.3	137.0	0.1	Plasma membrane	C05	18659840	18673533	+
BnaC06T0229400ZS	BnaC.PGP34	1255	33.2	6.5	136.3	0.2	Plasma membrane	C06	33969787	33975831	+
BnaC06T0234700ZS	BnaC.PGP35	1277	36.1	7.6	137.9	0.1	Plasma membrane	C06	34525466	34530347	-
BnaC07T0047900ZS	BnaC.PGP36	1222	34.5	7.8	132.7	0.2	Plasma membrane	C07	8046796	8052308	+
BnaC07T0312800ZS	BnaC.PGP37	1244	36.8	8.3	135.9	0.1	Plasma membrane	C07	45354192	45359844	-
BnaC07T0316300ZS	BnaC.PGP38	1144	34.4	8.7	124.6	0.1	Plasma membrane	C07	45777121	45783831	-
BnaC07T0324400ZS	BnaC.PGP39	1241	35.8	8.6	136.8	0.1	Plasma membrane	C07	46494268	46503682	+
BnaC07T0419700ZS	BnaC.PGP40	1257	37.5	6.8	136.2	0.1	Plasma membrane	C07	52888247	52893691	+
BnaC08T0001100ZS	BnaC.PGP41	1274	34.3	8.3	136.8	0.1	Plasma membrane	C08	147711	152335	+
BnaC09T0026900ZS	BnaC.PGP42	1155	38.2	8.5	126.3	0.1	Plasma membrane	C09	1776593	1782089	-
BnaC09T0240800ZS	BnaC.PGP43	1205	37.5	8.9	132.2	0.1	Plasma membrane	C09	22126416	22142968	-
Bnascaffold0024T0000200ZS	Bna.PGP44	1284	35.3	7.0	138.5	0.1	Plasma membrane	scaffold0024	5473	10892	+
Bnascaffold0027T0043600ZS	Bna.PGP45	1244	35.9	6.9	136.3	0.2	Plasma membrane	scaffold0027	3810661	3817759	+
Bnascaffold0287T0000200ZS	Bna.PGP46	1150	35.2	6.4	125.9	0.1	Plasma membrane	scaffold0287	6309	11643	-
Bnascaffold0383T0000200ZS	Bna.PGP47	1249	35.6	6.7	136.8	0.2	Plasma membrane	scaffold0383	4471	11456	-
Bnascaffold2856T0000100ZS	Bna.PGP48	1249	35.6	6.7	136.8	0.2	Plasma membrane	scaffold2856	1001	7983	-

*Isoelectric Point

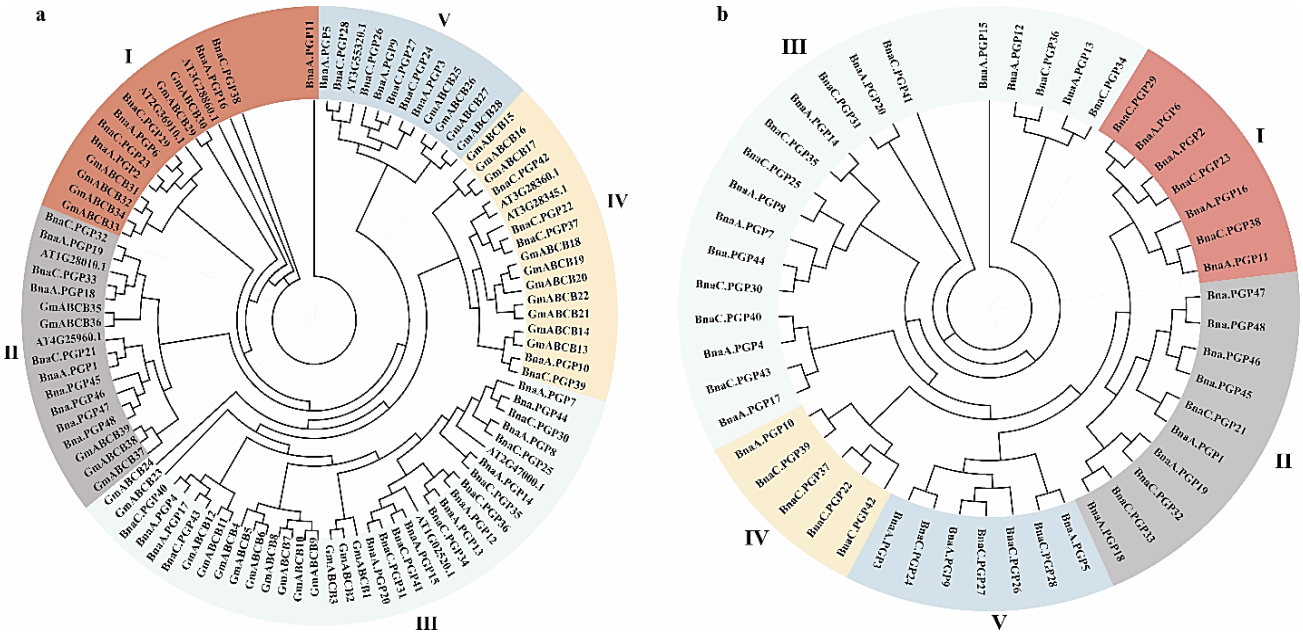

Fig. 1. Phylogenetic tree of *PGP* protein sequences in rapeseed, Arabidopsis, and soybean. An unrooted phylogeny was constructed using IQTREE with maximum likelihood, and the bootstrap was set at 1000 replicates. All PGP proteins are clustered into five phylogenetic clades, named I to V, each with a varying number of members from the selected species.

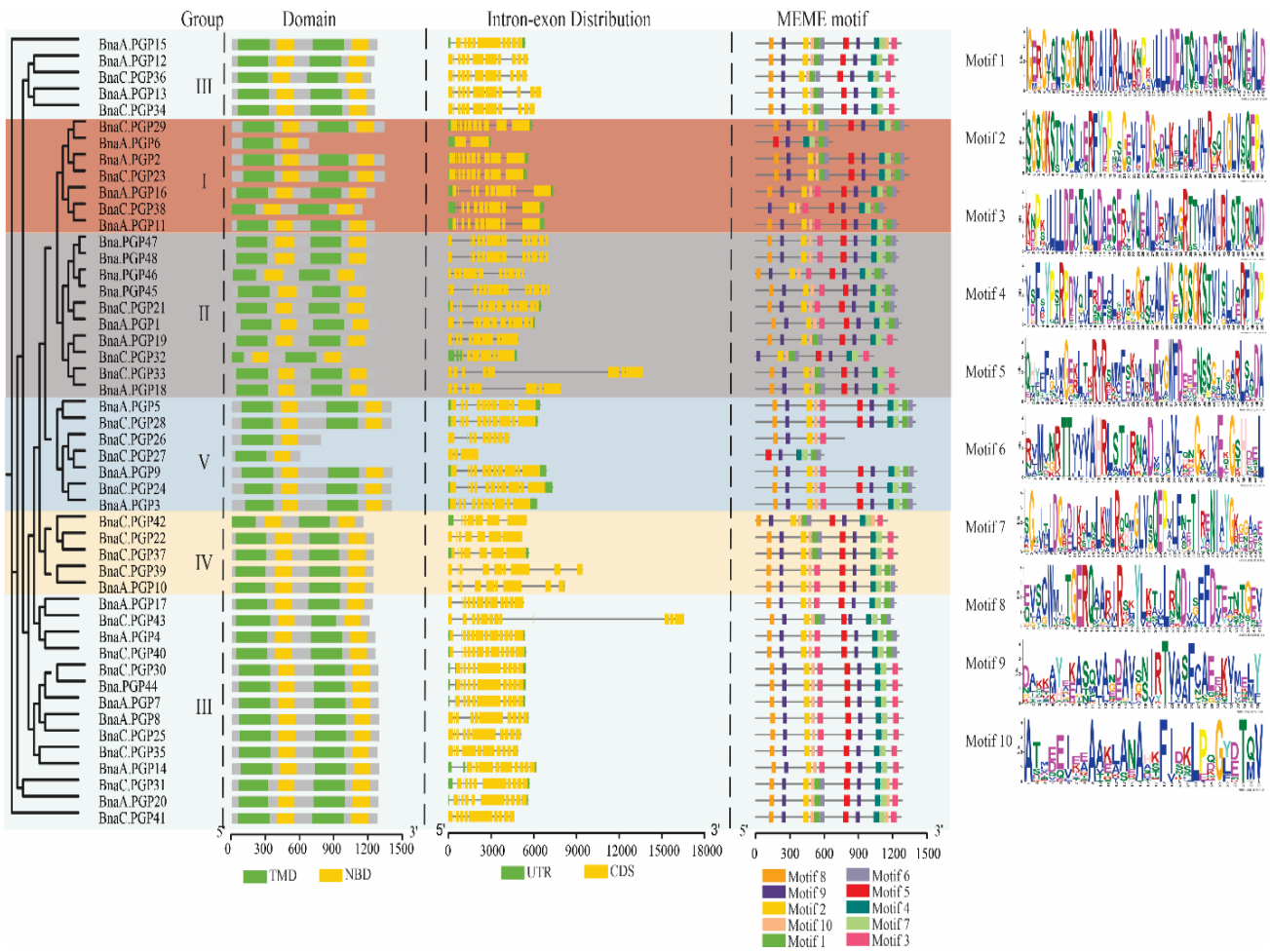

Fig. 2. Schematic representation of *PGP* domains, intron–exon structures, and conserved motifs of *BnaPGP* genes. The phylogenetic relationships among *BnaPGP* proteins were constructed using MEGA 7, which classified them into five distinct groups (I–V). The positional arrangements of the peripheral nucleotide-binding domain (NBD) and hydrophobic transmembrane domain (TMD) are shown for each *BnaPGP* protein. Gene structure analysis illustrated the distribution of exons, introns, and untranslated regions (UTRs), where exons, introns, and 3′/5′ UTRs are represented by orange boxes, black lines, and green boxes, respectively. Conserved motifs were identified using the MEME Suite and visualized using TBtools, with ten motifs represented by different colored boxes.

Table 3. Gene duplication events predicted in rapeseed.

Seq_1	Seq_2	Ka	Ks	Ka_Ks	Time (MYA)	Selection type
BnaA.PGP1	BnaC.PGP21	0.00321	0.10665	0.03013	35.54976322	Purifying
BnaA.PGP2	BnaA.PGP6	0.04026	0.47983	0.0839	159.9446642	Purifying
BnaA.PGP2	BnaC.PGP23	6.56E-04	0.12567	0.00522	41.88877167	Purifying
BnaA.PGP2	BnaC.PGP29	0.02239	0.41955	0.05337	139.8501384	Purifying
BnaA.PGP3	BnaA.PGP9	0.02265	0.28299	0.08003	94.33098328	Purifying
BnaA.PGP3	BnaC.PGP24	0.00536	0.09959	0.05387	33.19689005	Purifying
BnaA.PGP4	BnaC.PGP40	0.00419	0.10904	0.03839	36.34778488	Purifying
BnaA.PGP5	BnaC.PGP28	0.01043	0.12093	0.08627	40.31137433	Purifying
BnaA.PGP6	BnaC.PGP29	0.01726	0.02835	0.60876	9.449585259	Purifying
BnaA.PGP7	BnaA.PGP8	0.02722	0.38108	0.07144	127.0270577	Purifying
BnaA.PGP7	BnaC.PGP30	0.0065	0.14513	0.0448	48.3767776	Purifying
BnaA.PGP7	BnaC.PGP25	0.02315	0.37141	0.06233	123.8042815	Purifying
BnaA.PGP9	BnaC.PGP24	0.02187	0.26064	0.08393	86.87918967	Purifying
BnaA.PGP9	BnaC.PGP26	0.01749	0.14158	0.12353	47.19471826	Purifying
BnaA.PGP10	BnaC.PGP39	0.01084	0.10794	0.10047	35.98050979	Purifying
BnaA.PGP11	BnaA.PGP16	0.01421	0.4591	0.03095	153.0344048	Purifying
BnaA.PGP12	BnaC.PGP36	0.01674	0.04533	0.36939	15.10943705	Purifying
BnaA.PGP13	BnaC.PGP34	0.00878	0.04354	0.20171	14.51204344	Purifying
BnaA.PGP14	BnaC.PGP35	0.0069	0.13188	0.0523	43.96044471	Purifying
BnaA.PGP15	BnaA.PGP20	0.04039	0.50411	0.08012	168.0373372	Purifying
BnaA.PGP15	BnaC.PGP31	0.04094	0.50304	0.08138	167.6813808	Purifying
BnaA.PGP15	BnaC.PGP41	0.00571	0.17234	0.03314	57.44626786	Purifying
BnaA.PGP17	BnaC.PGP43	0.03917	0.08317	0.47091	27.72481288	Purifying
BnaA.PGP18	BnaC.PGP33	0.01199	0.05611	0.21366	18.703874	Purifying
BnaA.PGP19	BnaC.PGP32	0.01163	0.16877	0.06894	56.25583876	Purifying
BnaA.PGP20	BnaC.PGP31	0.00652	0.10165	0.06415	33.88492098	Purifying
BnaA.PGP20	BnaC.PGP41	0.04064	0.527	0.07711	175.6651519	Purifying
BnaC.PGP22	BnaC.PGP37	0.04211	0.35631	0.11818	118.769297	Purifying
BnaC.PGP23	BnaC.PGP29	0.02279	0.4314	0.05284	143.8012181	Purifying
BnaC.PGP24	BnaC.PGP26	0.035	0.26509	0.13202	88.36302263	Purifying
BnaC.PGP31	BnaC.PGP41	0.04101	0.52232	0.07851	174.1072152	Purifying

Time= Ks/2R, R= 1.5e-8

Prediction of CAREs within the promoter regions of *BnaPGPs*: The promoter sequence of 2000 bp upstream of the ATG start codon in all *BnaPGP* genes revealed the identification of 50 functional CAREs, primarily related to plant growth and development, stress adaptation, and hormone responses (Fig. 3). Among these CAREs involved in plant growth, development, and light-responsive elements were the most abundant (G-box, ACE, Sp1, and GT1-motif), representing approximately 50% of all elements. Few hormone-related CAREs were detected, including abscisic acid-responsive elements (ABREs), gibberellin-responsive elements (GARE motif, TATC-box, P-box), auxin-responsive elements (AuxRR core, TGA element), salicylic acid-responsive elements (TCA element), and methyl jasmonate-responsive elements (CGTCA motif and TGACG motif). Among these hormone-responsive elements, JA-related elements were the most numerous (69), followed by ABA-responsive elements (41), and gibberellin-responsive elements (29). *BnaC.PGP21* contained 22 TGACG motifs, *BnaA.PGP12*, *BnaA.PGP14*, *BnaA.PGP16*, *BnaC.PGP24*, *BnaC.PGP26*, *BnaC.PGP35* and *BnaC.PGP36* contained six *BnaA.PGP9* contained five, and the remaining. In addition, several stress-related CAREs were detected, including low-temperature-responsive elements (LTRs), MBS elements, and TC-rich repeats that can bind to drought-inducible MYB transcription factors. Pi is a major limiting factor in plant growth, development, and productivity. Phosphate starvation response 1 (PHR1) is a binding site (P1BS, GNATATNC) dimer that binds to an imperfect palindromic sequence. P1BS were found in the promoters of the BnaPGP genes *BnaA.PGP6* and *BnaA.PGP16* in clade I, *BnaA.PGP21* and *BnaA.PGP33* in clade II, *BnaA.PGP15*, *BnaA.PGP12*, *BnaC.PGP36*, *BnaA.PGP17*, *BnaC.PGP40*, *BnaC.PGP30*, and *BnaC.PGP44* in clade III; *BnaC.PGP22*, *BnaC.PGP33*. *BnaC.PGP39* and *BnaC.PGP10* in clade. These results indicate an effect occurring downstream in the Pi starvation signaling pathway (Fig. 3).

Chromosomal mapping and gene duplication events of the *BnaPGP* family members: The location of the 48 *BnaPGP* transport genes encoding the ABCB protein family on the chromosomes of the rapeseed genome was assessed. All *BnaPGP* proteins were distributed on 19 chromosomes, excluding *Bna.PGP44*, *Bna.PGP45*, *Bna.PGP46*, *Bna.PGP47*, and *Bna.PGP48* on scaffolds, which were later assigned to their original positions in the rapeseed genome. We found that more genes are present in sub-genome C (23 *PGP* members) compared with 20 members in sub-genome A. For instance, four genes (*BnaA.PGP16–BnaA.PGP19*) on Chromosome A09, three genes on Chromosome A03 (*BnaA.PGP2–BnaA.PGP4*), Chromosome A04 (*BnaA.PGP5-BnaA.PGP7*), Chromosome A07 (*BnaA.PGP12–BnaA.PGP14*), A05 (*BnaA.PGP8–BnaA.PGP9*), A06 (*BnaA.PGP10–BnaA.PGP11*), Chromosome A01, A08, and A10 contained single genes each in sub-genome A. For *PGP* family members located on sub-genome C include six genes (*BnaC.PGP25–BnaC.PGP30*) were located on Chromosome C04, five genes (*BnaC.PGP36–BnaC.PGP40*) on chromosomes C07, three genes on Chromosome C05 (*BnaC.PGP32–BnaC.PGP33*), two genes on Chromosome C03 (*BnaC.PGP23–BnaC.PGP24*), C06 (*BnaC.PGP34–BnaC.PGP35*), C09 (*BnaC.PGP42–BnaC.PGP43*) each. Chromosomes C01, C02, and C08 had a single PGP member each (Fig. 4a).

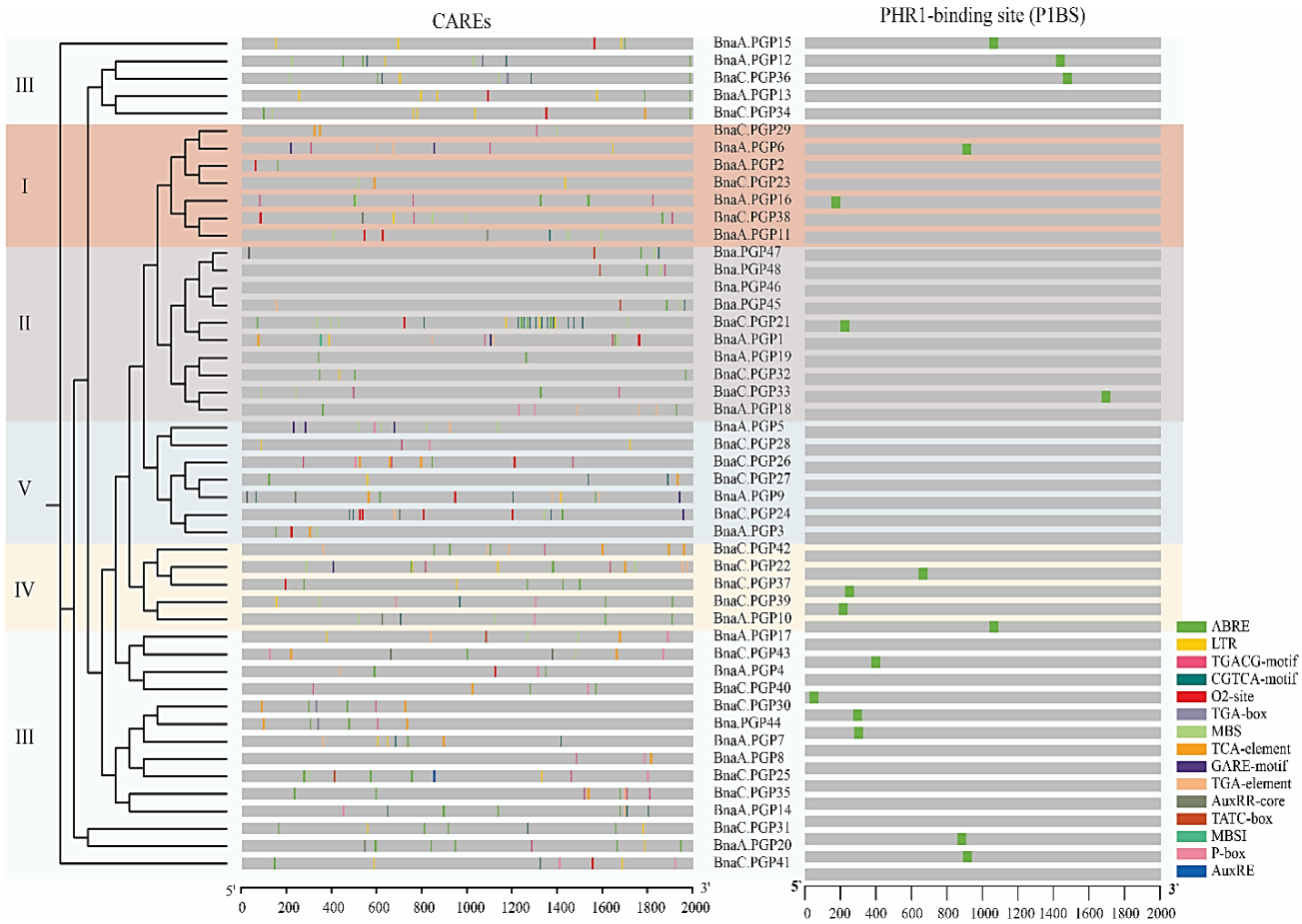

Fig. 3. Enrichment of *cis*-acting regulatory elements (CAREs) and Phosphate Starvation Response 1 (PHR1) binding sites (P1SB) in the 2 kb promoter regions of PGP family genes in rapeseed. The distribution of selected cis-acting elements across the promoters of the 48 *BnaPGP* genes is illustrated.

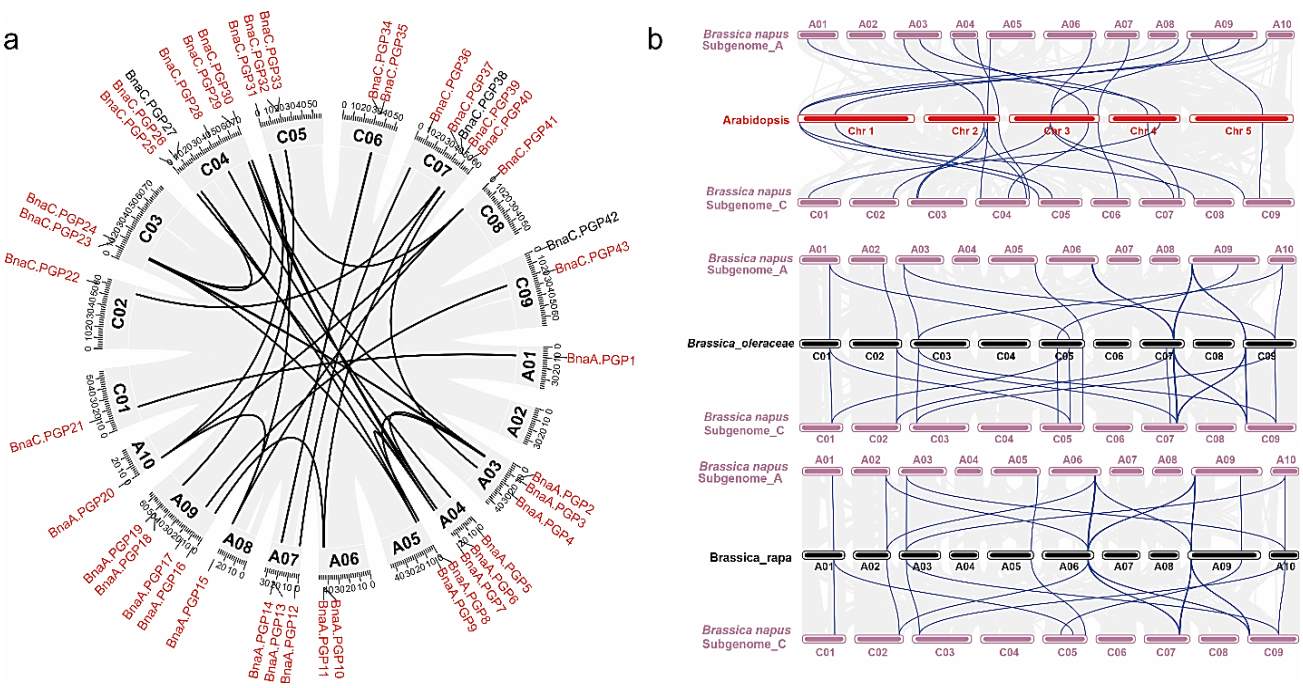

Fig. 4. Chromosomal location and duplication events of *BnaPGP* genes in rapeseed.
(a) Schematic representation of the chromosomal distribution and interchromosomal relationships of *BnaPGP* genes. Segmental duplication events are indicated by black lines connecting gene pairs labeled in red, whereas genes without identified duplications are labeled in black. Chromosome numbers are shown at the base of each chromosome. **(b)** Synteny analysis of *PGP* genes among *Brassica napus*, *B. rapa*, *B. oleracea*, and *Arabidopsis thaliana*. The blue lines indicate syntenic gene pairs, illustrating conserved genomic regions across species.

Table 4. Collinearity analysis of *BnaPGP* genes in *Brassica napus, Arabidospsis, Brassica rapa, and Brassica oleraceae*.

Brassica napus	*Arabidopsis*	*Brassica oleracea*	*Brassica rapa*
BnaA.PGP1	AT4G25960.1	-	BraA01g016810.4C.1, BraA03g054260.4C.1
BnaA.PGP2	AT2G36910.1	-	BraA03g019520.4C.1, BraA04g028440.4C.1
BnaA.PGP3	-		BraA03g021290.4C.1, BraA05g006670.4C.1
BnaA.PGP4	AT4G18050.1	-	BraA03g049080.4C.1
BnaA.PGP5	AT3G55320.1	-	BraA04g004890.4C.1
BnaA.PGP6	-		BraA03g019520.4C.1, BraA04g028440.4C.1
BnaA.PGP7	AT2G47000.1	-	BraA04g034640.4C.1, BraA05g000980.4C.1
BnaA.PGP8	-		BraA04g034640.4C.1, BraA05g000980.4C.1
BnaA.PGP9	AT2G39480.1	-	BraA03g021290.4C.1, BraA05g006670.4C.1
BnaA.PGP10	-		BraA06g038550.4C.1
BnaA.PGP11	AT3G28860.1	-	BraA02g040150.4C.1, BraA06g039260.4C.1, BraA09g003910.4C.1
BnaA.PGP12	-	-	BraA07g003090.4C.1
BnaA.PGP13	-	-	BraA07g025660.4C.1
BnaA.PGP14	AT3G62150.1	-	BraA07g026160.4C.1
BnaA.PGP15	AT1G02520.1	-	BraA08g036660.4C.1, BraA10g001290.4C.1
BnaA.PGP16	AT3G28860.1	-	BraA06g039260.4C.1, BraA09g003910.4C.1
BnaA.PGP17	AT5G46540.1	-	BraA09g023110.4C.1
BnaA.PGP18	AT1G28010.1	-	BraA09g039550.4C.1
BnaA.PGP19	AT1G27940.1	-	BraA09g039630.4C.1
BnaA.PGP20	AT1G02520.1	-	BraA08g036660.4C.1, BraA10g001290.4C.1
BnaC.PGP21	AT4G25960.1	BolC01g020450.2J.m1, BolC07g052470.2J.m1	-
BnaC.PGP22	AT3G28345.1	BolC02g053960.2J.m1, BolC07g035870.2J.m1	-
BnaC.PGP23	AT2G36910.1	BolC03g021750.2J.m1, BolC04g061940.2J.m1	-
BnaC.PGP24	AT2G39480.1	BolC03g023860.2J.m1, BolC04g008500.2J.m1	-
BnaC.PGP25	-	BolC04g001650.2J.m1	-
BnaC.PGP26	AT2G39480.1	-	-
BnaC.PGP27	-	BolC03g023860.2J.m1, BolC04g008500.2J.m1	-
BnaC.PGP28	AT3G55320.1	BolC04g036740.2J.m1	-
BnaC.PGP29	AT2G36910.1	BolC03g021750.2J.m1, BolC04g061940.2J.m1	-
BnaC.PGP30	AT2G47000.1	BolC04g001300.2J.m1, BolC04g001650.2J.m1, BolC04g068310.2J.m1	-
BnaC.PGP31	AT1G02520.1	BolC05g001220.2J.m1, BolC08g000090.2J.m1	-
BnaC.PGP32	AT1G27940.1	BolC05g025430.2J.m1	-
BnaC.PGP33	AT1G28010.1	BolC05g025550.2J.m1, BolC06g026160.2J.m1	-
BnaC.PGP35	AT3G62150.1	BolC06g026910.2J.m1	-
BnaC.PGP37	AT3G28345.1	BolC02g053960.2J.m1, BolC07g035870.2J.m1	-
BnaC.PGP39	-	BolC07g037070.2J.m1	-
BnaC.PGP40	AT4G18050.1	BolC07g047480.2J.m1	-
BnaC.PGP41	AT1G02520.1	BolC05g001220.2J.m1, BolC08g000090.2J.m1	-
BnaC.PGP42	AT3G28390.1	BolC07g035910.2J.m1, BolC09g003630.2J.m1	-
BnaC.PGP43	AT5G46540.1	BolC09g026030.2J.m1	-

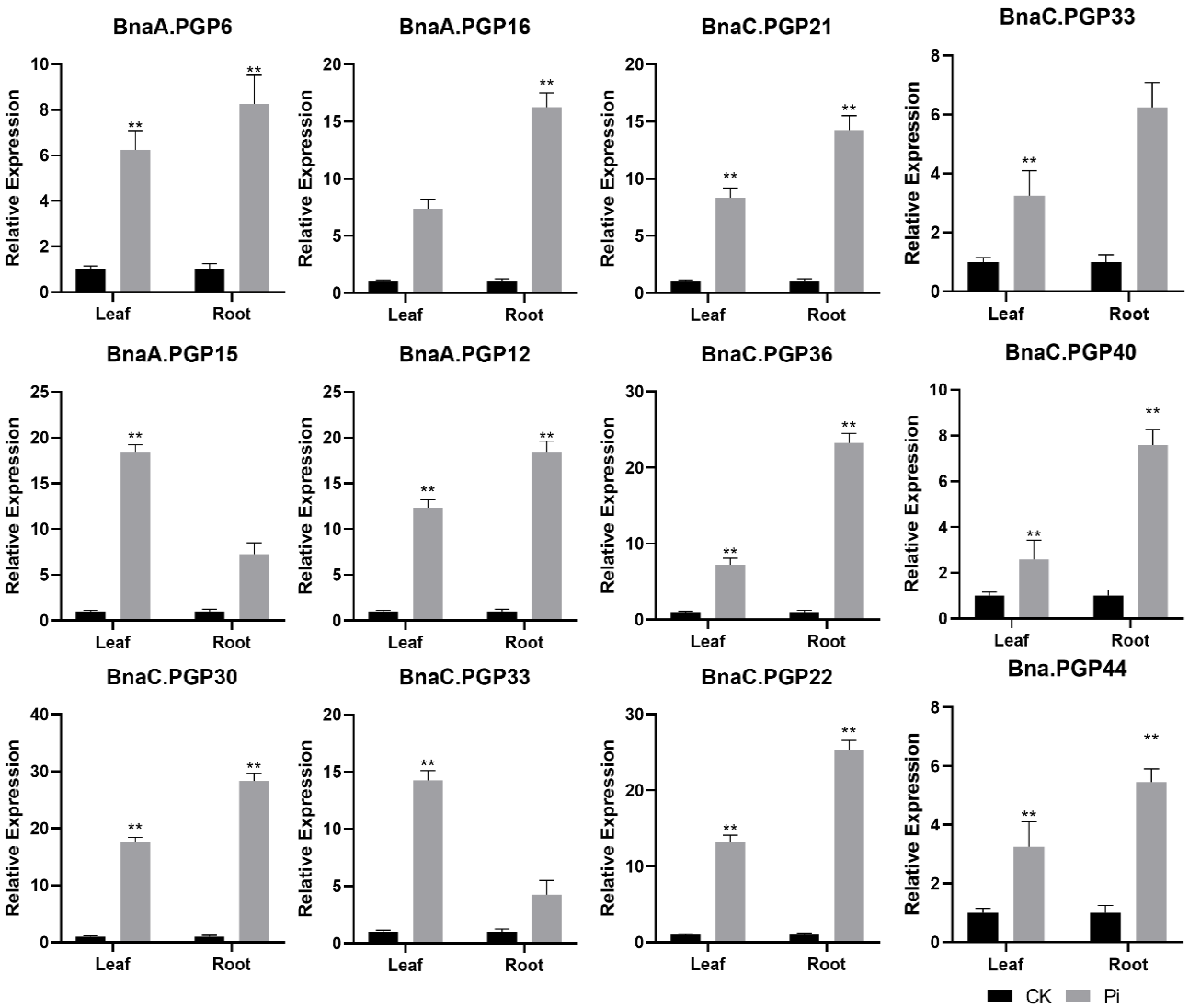

Fig. 5. Expression patterns of *BnaPGP* genes in response to low Pi conditions. RT-qPCR was used to determine the expression levels of *BnaPGP* genes.* indicate level of significance calculated with student's t-test.

To study *PGP* duplication on each chromosome, an intraspecific collinearity analysis showed that there were 31 pairs of segmental duplication events involving 41 *BnaPGP* family members. However, no tandem duplication events were detected, indicating that segmental replication events play a major role in the expansion of the *BnaPGP* family in rapeseed (Fig. 4a). The Ka/Ks ratios of all the duplication events were less than 1 (Table 3), indicating that purifying selection, which can keep the gene stable and preserve its function, occurred in the *BnaPGP* family during the evolutionary process. We also analyzed the interspecies collinearity map involving *Arabidopsis*, *B. rapa*, and *B. oleracea*. The results indicated that the 30, 32, and 32 *BnaPGP* genes were collinear with the genes in the *Arabidopsis*, *B. rapa*, and *B. oleracea* genomes, respectively (Fig. 4b and Table 4).

Expression analysis of *BnaPGPs* under Pi starvation: To understand the regulatory role of *BnaPGP* in rapeseed, we selected *BnaPGP* genes based on the presence of Pi-responsive *cis*-acting regulatory elements (e.g., P1BS) in their promoter regions to assess the expression patterns of *BnaPGP* proteins under Pi starvation. The results revealed significant differences in the responses of *BnaPGP* genes to Pi starvation (Fig. 5). *BnaA.PGP15* and *BnaC.PGP33* was upregulated in the *BnaA.PGP6*, *BnaA.PGP16*, *BnaA.PGP6*, *BnaC.PGP33*, *BnaA.PGP12*, *BnaC.PGP36*, *BnaC.PGP40*, *BnaC.PGP30*, *Bna.PGP22*, and *Bna.PGP44* was expressed significantly in roots, indicating its role in root.

Discussion

Phosphorus is one of the essential macronutrients required for plant growth, development, and yield (Aslam *et al.*, 2019). Studies have shown that in barley and wheat, a rhizosphere with longer root hairs confers a competitive advantage in Pi acquisition, alleviating physiological stress under conditions of Pi deficiency (Brown *et al.*, 2012). The membrane proteins of Class ATP-binding cassette (ABC) transporters are widely found in plants. These transporters play a multi-level regulatory role and are responsible for the transmembrane transport of various substrates, including P during Pi starvation (Aslam *et al.*, 2021; Devi *et al.*, 2024). Although their functions are less studied than those of classic P transporters (such as PHT1), they are gradually gaining attention. Previous studies have reported

that in white lupin, the *L.albABCG37* gene regulates indolebutyric acid (IBA) transport, inducing clustered root formation, and thus promoting Pi acquisition (Xu *et al.*, 2020). However, Aslam *et al*., (2021) reported the role of *L.albABCG29* in improving P use in white lupins. Numerous studies have shown that rice biomass and yield are critically dependent on Pi availability in acidic soils (Dogbe *et al.*, 2015). Rapeseed growth is highly sensitive to the supply of multiple key chemical elements and is particularly sensitive to Pi deficiency. Applying Pi fertilizer not only significantly promotes plant growth and yield but also increases Pi accumulation and oleic acid content during seed maturation (Li *et al.*, 2005; Liu *et al.*, 2024). However, current research on the functional roles of genes regulating phosphorus uptake efficiency in rapeseed remains limited. PHT1 genes have been identified and functionally analyzed in rapeseed (Li *et al*., 2019). Studies have shown that genes such as *BnPT10*, *BnPT11*, and *BnPT35* play an important role in the positive regulation of phosphorus absorption (Zhang *et al.*, 2025a). However, studies on Pi starvation in *B. napus* have been limited.

The ABC transporter family is generally divided into multiple subfamilies, including ABCA to ABCI, based on structural characteristics and sequence similarities (Kang *et al*., 2011). The present study reports the bioinformatics identification of the ABC transport protein subfamily PGP in rapeseed. The number of PGP proteins varies among different species, for instance, *Arabidopsis* (28 members) (Jasinski *et al.*, 2003), *B. rapa* (39 members) (Yan *et al.*, 2017), *P. ostii* (29 members) (Shang *et al*., 2025), rice (22 members) (Xu *et al.*, 2014b), *G. glabra* contained 45 members (Devi *et al.*, 2024), soybean (39 genes) (Zou *et al.*, 2025), grapevine (19 members) (Çakır *et al*., 2023), maize (31 members) (Pang *et al.*, 2013), *L. usitatissimum* (48 genes) (Khan *et al*., 2020), and tomatoes (29 members) (Ofori *et al.*, 2018). In *B. napus*, 48 PGP proteins were identified (Table 1), which is higher than that in any plant species reported to date. This higher number of *PGP* genes in rapeseed indicates that, overall, the loss and gain of genes and replication among different species tend to stability.

Chromosome localization and phylogeny revealed that the *BnaPGP* transporter gene family members in *B. napus* are distributed across all chromosomes. Collinearity analysis revealed that collinearity between *B. napus* and *Arabidopsis* was higher than that between *B. napus* and *B. rapa* or *B. oleracea*. This discrepancy may be due to differences in genomic structure and organization between species. The diversity of gene structure, particularly the distribution of introns and exons, helps reveal the phylogenetic relationships of gene families. This study found that the number of introns in the *BnaPGP* gene family ranges from 2 to 12, and that the intron/exon structure is similar across subfamilies. Phylogenetic and conserved sequence analysis has divided *BnaPGP* proteins into five distinct groups, all of which are full-size *BnaPGP* transporters. Previous studies have shown that full-length *PGP* transporters can mediate the transport of various substrates, including lipoproteins, fungicides, peptides, cell surface components, and auxins (Kim *et al.*, 2006b). This functional property suggests that the *BnaPGP* transporter family may play a key role in the response to Pi starvation stress.

In recent years, a growing number of studies have demonstrated that ABCB genes also play an important role in plant responses to Pi starvation (Devi *et al.*, 2024). Although their role is not directly involved in Pi transport, they have potential regulatory value in the development of plant adaptation to low Pi conditions by influencing root structural remodeling, hormone polarity transport, and stress signaling (Waseem *et al.*, 2026). First, the changes in root morphology caused by Pi starvation are an important mechanism for improving the Pi acquisition capacity (Aslam *et al.*, 2021). Studies have shown that under low-Pi conditions, plants usually inhibit the elongation of the main root and enhance the formation of lateral roots and root hair development, thereby expanding the root absorption surface area (Xu *et al.*, 2020). ABCB transporters (such as ABCB1 and ABCB19) are widely involved in the regulation of polar auxin transport and are important regulatory factors for maintaining root polar development (Chen *et al.*, 2025). Second, ABCB genes may play a role in coordinating stress signals and hormone interactions. Pi starvation is often accompanied by the redistribution of other nutrients, such as iron and zinc, and changes in redox status, processes that involve complex signaling and regulatory networks. Previous studies have shown that certain ABC transporters, such as the ALS3-STAR1 complex, mediate the inhibition of primary root growth by regulating iron homeostasis under Pi deficiency (Wang *et al.*, 2019). This at ABC transporters may play a key role in cross-nutrient responses and signal transduction. The present study involved genomic analyses of the *PGP* family in rapeseed, revealing a large and diverse membership with distinct expression under Pi starvation. The *BnaAPGP* genes were upregulated under low-P stress, suggesting their potential involvement in regulating physiological processes associated with P starvation. However, the direct molecular functions of PGP transporters in P stress responses remain largely unexplored, particularly with respect to substrate recognition, expression regulation, and interactions with canonical P-transport systems.

Conclusion

This study systematically identified the *PGP* transporter subfamily in rapeseed, discovering a total of 48 *BnaPGP* genes. A comprehensive analysis was conducted on their gene structure, conserved motifs, chromosomal distribution, evolutionary relationships, and CAREs. Phylogenetic results divided these genes into five clades, revealing that gene expansion is primarily driven by segment duplication. CAREs analysis showed that various hormone and stress-related regulatory elements are widely present in the promoter regions of *BnaPGP* genes, including the P1BS element in response to P deficiency signals, suggesting that these genes may participate in complex regulatory networks. Under low P treatment conditions, few *BnaPGP* genes were significantly upregulated in the roots, indicating that they may participate in root remodeling and P uptake adaptation responses by regulating polar growth and hormone transport. This study fills the gap in the systematic identification and functional prediction of *ABCB/PGP* genes in rapeseed and also provides important genetic resources and a theoretical foundation for further functional verification and the breeding of high-P-utilizing rapeseed varieties.

Acknowledgments

This work was supported by grants from the China NSFC Research Fund for International Young Scientists (grant number: 32250410291), the Scientific Research Start-up Funding Project of Hainan University (Grant No. XJ2500000633), the Key Research Program of Hainan Province (grant number: ZDYF2022XDNY185), and a Special Project for the Academician Team Innovation Center of Hainan Province (grant number: YSPTZX202206). We also sincerely thank our colleague Dr. Enerand Mackon at the School of Breeding and Multiplication (Sanya Institute of Breeding and Multiplication), School of Tropical Agriculture and Forestry, Hainan University, Sanya, China, for proofreading and language editing the manuscript.

Author's Contribution SB: Analyzed the data, wrote the manuscript. WH: analyzed the data, wrote the manuscript. ZP: analyzed the data. MH: analyzed the data. WM: analyzed the data, wrote the manuscript, Review the manuscript. PL: Review the manuscript. All authors read and approved the final version.

Conflict of Interest The authors declare that they have no known competing financial interests or personal relationships that could have appeared to influence the work reported in this paper.

Funding: This work was supported by grants from the China NSFC Research Fund for International Young Scientists (grant number: 32250410291), the Scientific Research Start-up Funding Project of Hainan University (Grant No. XJ2500000633), the Key Research Program of Hainan Province (grant number: ZDYF2022XDNY185), and a Special Project for the Academician Team Innovation Center of Hainan Province (grant number: YSPTZX202206).

References

Adu, M.O., D.O. Yawson, M.J. Bennett, M.R. Broadley, L.X. Dupuy and P.J. White. 2017. A scanner-based rhizobox system enabling the quantification of root system development and response of *Brassica rapa* seedlings to external p availability. *Plant Root*, 11: 16-32.

Aslam, M.M., J. Karanja and S.K. Bello. 2019. *Piriformospora indica* colonization reprograms plants to improved p-uptake, enhanced crop performance, and biotic/abiotic stress tolerance. *Physiol. Mol. Plant Pathol.*, 106: 232-237.

Aslam, M.M., M. Waseem, Q. Zhang, W. Ke, J. Zhang and W. Xu. 2021. Identification of ABC transporter g subfamily in white lupin and functional characterization of *L.albABGC29* in phosphorus use. *BMC Genom.*, 22(1): 723.

Blakeslee, J.J., A. Bandyopadhyay, O.R. Lee, J. Mravec, B. Titapiwatanakun, M. Sauer, S.N. Makam, Y. Cheng, R. Bouchard, J. Adamec. 2007. Interactions among pin-formed and p-glycoprotein auxin transporters in *Arabidopsis*. *Plant Cell*, 19(1): 131-147.

Brown, L.K., T.S. George, J.A. Thompson, G. Wright, J. Lyon, L. Dupuy, S.F. Hubbard and P.J. White. 2012. What are the implications of variation in root hair length on tolerance to phosphorus deficiency in combination with water stress in barley (*Hordeum vulgare*)?. *Ann. Bot.*, 110(2): 319-328.

Çakır, B., H. Jalili and G. Turgay. 2023. Genome-wide analysis of the ABCB gene family in *Vitis vinifera*: Its expression patterns in berries and its responses to iron and heavy metal stresses. *J. Hort. Sci., Biotechnol.*, 98(5): 591-607.

Chen, Q., L. Zhu, S. Zhang, S. Qiao, Z.J. Ding, S.J. Zheng, J. Guo and N. Su. 2025. Structures and mechanisms of the ABC transporter abcb1 from *Arabidopsis thaliana*. *Structure*, 33(5): 903-915.

Dahuja, A., R.R. Kumar, A. Sakhare, A. Watts, B. Singh, S. Goswami, A. Sachdev and S. Praveen. 2021. Role of ATP-binding cassette transporters in maintaining plant homeostasis under abiotic and biotic stresses. *Physiol. Plant.*, 171(4): 785-801.

Devi, R., P. Goyal, B. Verma, S. Hussain, F. Chowdhary, P. Arora and S. Gupta. 2024. A transcriptome-wide identification of ATP-binding cassette (ABC) transporters revealed participation of ABCB subfamily in abiotic stress management of *Glycyrrhiza glabra L. BMC Genom.*, 25(1): 315.

Dogbe, W., J.M. Sogbedji and S.S.J. Buah. 2015. Site-specific nutrient management for lowland rice in the Northern Savannah Zones of Ghana. *Curr. World Environ.*, 3(2): 109-117.

Duan, X., K. Jin, G. Ding, C. Wang, H. Cai, S. Wang, P.J. White, F. Xu and L. Shi. 2020. The impact of different morphological and biochemical root traits on phosphorus acquisition and seed yield of *Brassica napus*. *Field Crops Res.*, 258: 107960.

Jasinski, M., E. Ducos, E. Martinoia and M. Boutry. 2003. The ATP-binding cassette transporters: Structure, function, and gene family comparison between rice and *Arabidopsis*. *Plant Physiol.*, 131(3): 1169-1177.

Jenness, M.K., N. Carraro, C.A. Pritchard and A.S. Murphy. 2020. Corrigendum: The *Arabidopsis* ATP-binding cassette transporter *ABCB21* regulates auxin levels in cotyledons, the root pericycle, and leaves. *Front. Plant Sci.*, 11: 351-369.

Kang, J., J.Y. Park, H. Choi, B. Burla, T. Kretzschmar, Y. Lee and E. Martinoia. 2011. Plant ABC transporters. *Arabidopsis Book*, 9(9): e0153.

Khan, N., F.M. You, R. Datla, S. Ravichandran, B. Jia and S. Cloutier. 2020. Genome-wide identification of ATP-binding cassette (ABC) transporter and heavy metal associated (HMA) gene families in flax (*Linum usitatissimum* L.). *BMC Genom.*, 21(1): 722.

Kim, D., L. Bovet, S. Kushnir, E.W. Noh, E. Martinoia and Y. Lee. 2006. *AtATM3* is involved in heavy metal resistance in *Arabidopsis*. *Plant Physiol.*, 140(3): 922-932.

Larsen, P.B., J. Cancel, M. Rounds and V.J.P. Ochoa. 2007. *Arabidopsis* als1 encodes a root tip and stele localized half type ABC transporter required for root growth in an aluminum toxic environment. 225(6): 1447-1458.

Li, Y., X. Wang, H. Zhang, S. Wang, X. Ye, L. Shi, F. Xu and G. Ding. 2019. Molecular identification of the phosphate transporter family 1 (PHT1) genes and their expression profiles in response to phosphorus deprivation and other abiotic stresses in *Brassica napus*. *PLoS One*, 14(7): e0220374.

Li, Y., X. Wang, H. Zhang, X. Ye, L. Shi, F. Xu and G. Ding. 2023. Phosphate transporter bnapt37 regulates phosphate homeostasis in *Brassica napus* by changing its translocation and distribution *in vivo*. *Plants*, 12(19): 3362.

Liu, C., Z. Bai, Y. Luo, Y. Zhang, Y. Wang, H. Liu, M. Luo, X. Huang, A. Chen and L. Ma. 2024. Multiomics dissection of *Brassica napus* L. Lateral roots and endophytes interactions under phosphorus starvation. *Nat. Comm.*, 15(1): 9732.

Livak, K.J. and T.D. Schmittgen. 2001. Analysis of relative gene expression data using real-time quantitative PCR and the 2(-Delta Delta C(T)) Method. *Methods*, 25(4): 402-408.

Multani, D.S., S.P. Briggs, M.A. Chamberlin, J.J. Blakeslee, A.S. Murphy and G.S. Johal. 2003. Loss of an *MDR* transporter in compact stalks of maize *br2* and sorghum *dw3* mutants. *Science*, 302(5642): 81-84.

Ofori, P.A., A. Mizuno, M. Suzuki, E. Martinoia, S. Reuscher, K. Aoki, D. Shibata, S. Otagaki, S. Matsumoto and K. Shiratake. 2018. Genome-wide analysis of ATP binding cassette (ABC) transporters in tomato. *PLoS One*, 13(7): e0200854.

Pang, K., Y. Li, M. Liu, Z. Meng and Y. Yu. 2013. Inventory and general analysis of the ATP-binding cassette (ABC) gene superfamily in maize (*Zea mays L.*). *Gene*, 526(2): 411-428.

Ren, F., Q-Q. Guo, L-L. Chang, L. Chen, C-Z. Zhao, H. Zhong and X-B. Li. 2012. *Brassica napus* PHR1 Gene Encoding a MYB-Like Protein Functions in Response to Phosphate Starvation. *Plos One* 7(8): e44005.

Saha, J., A. Sengupta, K. Gupta and B. Gupta. 2014. Molecular phylogenetic study and expression analysis of ATP-binding cassette transporter gene family in *Oryza sativa* in response to salt stress. *Comput. Biol. Chem.*, 54(NA): 18-32.

Santelia, D., V. Vincenzetti, E. Azzarello, L. Bovet, Y. Fukao, P. Düchtig, S. Mancuso, E. Martinoia and M. Geisler. 2005. MDR-like ABC transporter *AtPGP4* is involved in auxin-mediated lateral root and root hair development. *FEBS Lett.*, 579(24): 5399-5406.

Shang, W., C. Cui, X. Liu, W. Meng, Y. Qiu, Y. Sun, Y. Shen, W. Liu, Z. Wang and S. He. 2025. Genome-wide analysis of the ABCB family and its expression in adventitious root development of *Paeonia ostii*. *Horticulturae*, 11(2): 138.

Titapiwatanakun, B., J.J. Blakeslee, A. Bandyopadhyay, H. Yang, J. Mravec, M. Sauer, Y. Cheng, J. Adamec, A. Nagashima, M. Geisler et al. 2008. *ABCB19*/*PGP19* stabilises *PIN1* in membrane microdomains in *Arabidopsis*. *Plant J.*, 57(1): 27-44.

Wang, X., Z. Wang, Z. Zheng, J. Dong, L. Song, L. Sui, L. Nussaume, T. Desnos and D. Liu. 2019. Genetic dissection of Fe-dependent signaling in root developmental responses to phosphate deficiency. *Plant Physiol.*, 179(1): 300-316.

Waseem, M., S. Basharat, I. Shaheen and P. Liu. 2026. Genome-Wide Identification and Characterization of Long Non-Coding RNAs in Litchi. *Plant Sci. Horiz.*, 1(1): 12–21.

Xu, W., Q. Zhang, W. Yuan, F. Xu, M. Muhammad Aslam, R. Miao, Y. Li, Q. Wang, X. Li and X. Zhang. 2020. The genome evolution and low-phosphorus adaptation in white lupin. *Nat. Commun.*, 11: 1069.

Xu, Y., S. Zhang, H. Guo, S. Wang, L. Xu, C. Li, Q. Qian, F. Chen, M. Geisler and Y. Qi et al. 2014a. *OsABCB14* functions in auxin transport and iron homeostasis in rice (*Oryza sativa* L.). *Plant J.*, 79(1): 106-117.

Xu, Y.X., Y. Liu, S.T. Chen, X.Q. Li, L.G. Xu, Y.H. Qi, D.A. Jiang and S.H. Jin. 2014b. The b subfamily of plant ATP binding cassette transporters and their roles in auxin transport. *Biol. Plant.*, 58(3): 401-410.

Yan, C., W. Duan, S. Lyu, Y. Li and X. Hou. 2017. Genome-wide identification, evolution, and expression analysis of the ATP-binding cassette transporter gene family in *Brassica rapa*. *Front. Plant Sci.*, 8: 349.

Yang, G., G. Ding, L. Shi, H. Cai and F. Xu. 2012. Characterization of phosphorus starvation-induced gene *BnSPX3* in *Brassica napus*. *Plant Soil*, 350(1): 339-351.

Yue, R., Q. Sun, J. Ding, W. Li, W. Li, M. Zhao, S. Lu, T. Zeng, H. Zhang, S. Zhao al. 2022. Functional analysis revealed the involvement of *ZmABCB15* in resistance to rice black-streaked dwarf virus infection. *BMC Plant Biol.*, 22(1): 484.

Zhang, B., X. Zhu, P. Yuan, B. Han, T. Wu, I. Din, C. Wang, J.P. Hammond, S. Wang and G. Ding. 2025a. Root morphological adaptation and leaf lipid remobilization drive differences in phosphorus use efficiency in rapeseed seedlings. *Crop J.*, 13(2): 524-535.

Zhang, B., X. Zhu, P. Yuan, B. Han, T. Wu, I. Din, C. Wang, J.P. Hammond, S. Wang and G. Dingl. 2025b. Root morphological adaptation and leaf lipid remobilization drive differences in phosphorus use efficiency in rapeseed seedlings. *Crop J.*, 13(2): 524-535.

Zhang, B., Y. Wang, H. Liu, J. Wang, I. Din, J.P. Hammond, G. Ding, S. Wang, H. Cai and C. Wang. 2023. Effect of cultivars and nature–based solutions for the reduction of phosphate fertilizer usage on oilseed rape. *Field Crops Res.*, 293: 108851.

Zhang, Q., D. Xing, Y. Wu, K. Zhao, J. Wang and R. Mao. 2024. Effects of low-phosphorus stress on use of leaf intracellular water and nutrients, photosynthesis, and growth of *Brassica napus* L. *Horticulturae*, 10(8): 821.

Zhang, Y., V. Nasser, O. Pisanty, M. Omary, N. Wulff, M. Di Donato, I. Tal, F. Hauser, P. Hao, O. Roth et al. 2018. A transportome-scale amiRNA-based screen identifies redundant roles of *Arabidopsis ABCB6* and *ABCB20* in auxin transport. *Nat. Commun.*, 9(1): 4204-4204.

Zou, H., C. Fan, X. Chen, R. Chen, Z. Sun and X. Wan. 2025. Genome-wide analyses of the soybean GmABCB gene family in response to salt stress. *Genes*, 16(2): 233.